A Mode Shape Identification Method of Timber Pieces Based on Relative Rigid Displacement Decomposition

Panxu Sun,[a] Chen Ding,[a] Chongyang He,[b] Kaixuan Liang,[a,*] and Shuxia Wang [c]

As a commonly used method in the field of structural dynamic characteristics, mode shape identification currently relies largely on animation demonstrations of finite element modal analysis. This method is highly susceptible to the observer's perspective and subjective factors, making it difficult to accurately identify the mode shapes of timber pieces. To address this issue, the plane deformation decomposition theory of 2D-4 node quadrilateral elements was adopted to perform relative rigid body displacement decomposition on mode shapes, thereby achieving quantitative and visual identification of the overall mode shapes of timber pieces. The correctness of the proposed method was verified by comparison with the modal mass participation ratio method. In addition, this method can also determine the dominant rigid body displacement type of each element in the mode shapes of timber pieces, which highlights its superiority.

DOI: 10.15376/biores.21.2.4666-4677

Keywords: Timber pieces; Mode shape identification; Relative rigid body displacement decomposition

Contact information: a: School of Civil Engineering, Zhengzhou University, Zhengzhou, 450001, China; b: Henan Earthquake Agency, Zhengzhou 450018, China; c: School of Materials Science and Engineering, Zhengzhou University of Aeronautics, Zhengzhou 450046, China;
** Corresponding author: LiangKX0331@163.com*

INTRODUCTION

As a renewable and environmentally friendly building material, wood has unique advantages for modern construction, such as relatively low density, high strength, thermal insulation, and heat preservation (Ghiyasinasab *et al.* 2017; Augustino 2025). With the continuous development of timber structures, the safety, stability, and durability of timber pieces have attracted growing attention from designers and researchers (Gao *et al.* 2025). Conducting in-depth research on the accurate analysis and efficient evaluation of timber pieces performance is of great theoretical significance and engineering value.

Currently, the main research objects of building structural performance analysis are reinforced concrete members and steel members, for which relatively comprehensive theoretical systems and analysis methods have been established. In contrast, research on the performance of timber pieces is lagging, due to the material's inherent anisotropy (Perlin *et al.* 2019), natural defects (Zhao *et al.* 2024) (*e.g.*, knots and cracks), and the discreteness of its mechanical properties (Caprio and Jockwer 2026). Traditional methods for analyzing timber pieces performance mainly focus on conventional performance indicators such as strength, stiffness, and stability (Véliz *et al.* 2024; Ren *et al.* 2025; Sejkot *et al.* 2025).

However, obtaining these indicators often relies on the design of specific load cases. Both field loading tests and numerical simulation analyses require separate studies

for different load levels, load forms, and loading positions, which not only consume substantial human, material, and time costs but also struggle to fully cover the stress states of timber pieces in complex real-world environments. Moreover, irreversible damage may be inflicted on the pieces during the testing process (Renard *et al.* 2025).

As an analysis method based on structural dynamics, modal analysis boasts a core advantage: it is only related to the material properties, geometric shape, and boundary conditions of the structure, and it has no direct connection with external load cases. This characteristic enables it to break through the limitations of traditional analysis methods that depend on load design (Hamdi *et al.* 2021). In recent years, a series of advances have been made in the modal analysis of timber pieces in terms of natural frequencies, damping ratios, and mode shapes. Studies have shown that wood anisotropy, joint connection performance, and boundary constraints significantly affect the natural frequencies of structures, and variations in frequency can directly reflect changes in global stiffness (Cheraghi-Shirazi *et al.* 2025; Yassine and Mustapha 2024). The damping ratio of timber pieces is mainly influenced by factors such as material moisture content, wood defects, and ambient temperature and humidity, exhibiting obvious discreteness and frequency dependence, which can serve as an important basis for health monitoring (Jara-Cisterna *et al.* 2025; Amaddeo and Martinelli 2025). From a theoretical perspective, the deformation of a structure under any load can be expanded using mode shapes as a complete coordinate basis (Bracci and Kunnath 1997). This means that the mode shape information obtained through modal analysis can provide a comprehensive and universal foundation for describing the deformation laws of structures. The inherent structural characteristics contained in mode shapes can indirectly reflect the material uniformity, geometric integrity, and potential damage of timber pieces, allowing indirect evaluation of structural performance without the need for complex load application processes (Pan *et al.* 2023). This mode shape-based analysis approach can effectively reduce the workload of field tests and numerical simulations. In addition it can avoid the limitations caused by load case design, thus gradually demonstrating its potential in the performance analysis of timber pieces.

Wilson (2008) proposed the modal mass participation ratio method for quantitative mode shape identification, which determines the mode shape type by comparing the participation coefficient relationships of spatial structures or components in six degrees of freedom directions. Casalegno and Russo (2017) conducted experimental modal analysis on textile composite bridges, calculated key modal parameters, and compared the results with those obtained via the finite element method, yielding bending and torsional mode shapes with high-frequency and high-damping characteristics. Patil *et al.* (2018) proposed and verified a new method for obtaining a unified scaling factor, which can extract the mode shapes of complex structures using only a pair of cameras.

The rigid body displacement decomposition method has been applied to achieve quantitative mode shape analysis for concrete members (Sun *et al.* 2025). However, a suitable mode shape identification system has not yet been established for timber pieces, considering their dynamic characteristics of anisotropy, low stiffness, and high specific strength. The elastic modulus of wood is much lower than that of concrete and steel, resulting in low natural frequencies and a higher tendency to resonate under external loads (Xu *et al.* 2024). In addition, natural defects in wood lead to significant discreteness in dynamic properties, making traditional animation observation and the modal mass participation ratio method unable to meet the requirements of high-precision identification. Based on the deformation decomposition theory of 2D-4 node quadrilateral elements, this

paper proposes a relative rigid body displacement decomposition method suitable for timber pieces, which realizes quantitative and visual identification of mode shapes and compensates for the shortcomings of existing methods.

THEORETICAL BACKGROUND

The core objective of this paper was to construct basis matrices for rigid body displacements and fundamental deformations based on the plane deformation decomposition theory of 2D-4 node quadrilateral elements, decompose the mode shapes of timber pieces *via* relative rigid body displacement decomposition, and achieve quantitative mode shape identification as well as visual determination of the dominant displacement of each element.

The planar deformation of a 2D-4 node quadrilateral element can be divided into 3 kinds of rigid body displacement modes and 5 kinds of basic deformation modes, which are shown in Figs. 1 and 2, respectively (Sun *et al.* 2023). The rigid body displacement modes are composed of rigid body linear displacement in X, Y direction and rigid body rotational displacement in XOY plane, and the basic deformation modes are composed of tension-compression deformation and bending deformation in X, Y direction, and shearing deformation in XOY plane.

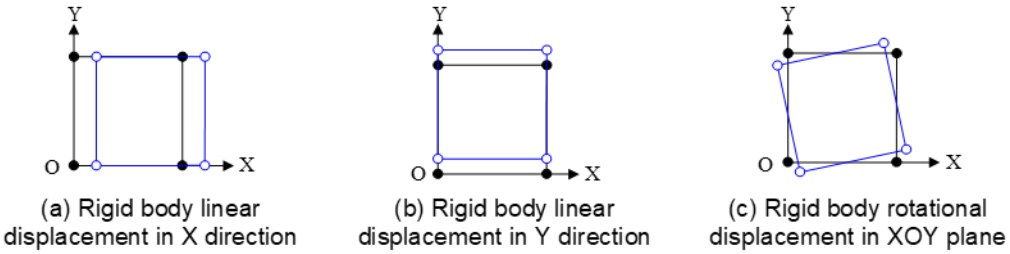

Fig. 1. Rigid body displacement modes of 2D-4 node quadrilateral element

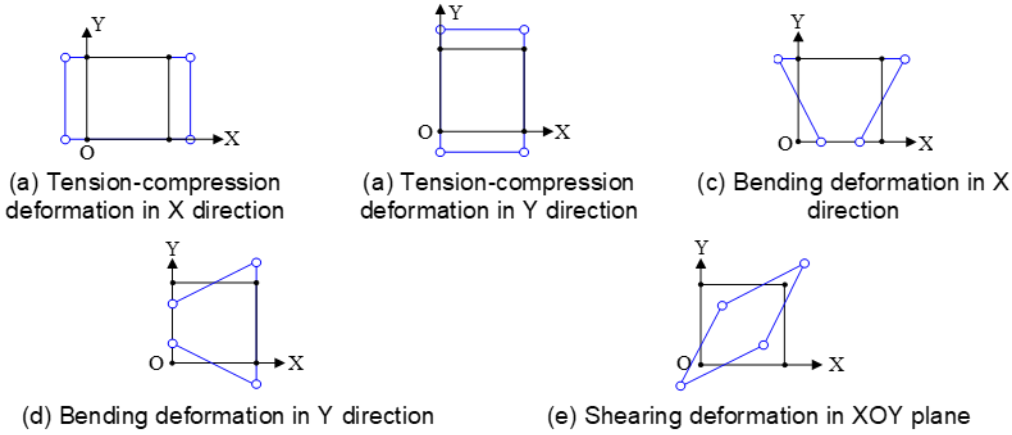

Fig. 2. Basic deformation modes of 2D-4 node quadrilateral element

Three base vectors of rigid body displacement modes and 5 base vectors of basic deformation modes of the 2D-4 node quadrilateral elements were constructed as follows,

$$\mathbf{B} = \begin{bmatrix} \mathbf{B}_r \\ \mathbf{B}_d \end{bmatrix} \tag{1}$$

where

$$\mathbf{B}_r = \begin{bmatrix} 0.5 & 0 & 0.5 & 0 & 0.5 & 0 & 0.5 & 0 \\ 0 & 0.5 & 0 & 0.5 & 0 & 0.5 & 0 & 0.5 \\ -0.3536 & 0.3536 & -0.3536 & -0.3536 & 0.3536 & -0.3536 & 0.3536 & 0.3536 \end{bmatrix} \tag{2}$$

$$\mathbf{B}_d = \begin{bmatrix} 0.5 & 0 & -0.5 & 0 & -0.5 & 0 & 0.5 & 0 \\ 0 & 0.5 & 0 & 0.5 & 0 & -0.5 & 0 & -0.5 \\ 0.5 & 0 & -0.5 & 0 & 0.5 & 0 & -0.5 & 0 \\ 0 & 0.5 & 0 & -0.5 & 0 & 0.5 & 0 & -0.5 \\ 0.3536 & 0.3536 & 0.3536 & -0.3536 & -0.3536 & -0.3536 & -0.3536 & 0.3536 \end{bmatrix} \tag{3}$$

where $\mathbf{B}_r$ and $\mathbf{B}_d$ are the base matrices of rigid body displacement modes and basic deformation modes, respectively. Row vectors from top to bottom in $\mathbf{B}_r$ are rigid body linear displacement in X and Y directions, and rigid body rotational displacement in XOY plane, respectively. Row vectors from top to bottom in $\mathbf{B}_d$ are tension-compression deformation in X and Y directions, bending deformation in X and Y direction, and shearing deformation in XOY plane, respectively.

The 2D-4 node quadrilateral elements were adopted to mesh the timber pieces and conduct modal analysis, and the relative displacement vector of the *k*-th element in the *j*-th mode shape is shown in Eq. 4

$$\boldsymbol{d} = (\Delta x_1 \quad \Delta y_1 \quad \Delta x_2 \quad \Delta y_2 \quad \Delta x_3 \quad \Delta y_3 \quad \Delta x_4 \quad \Delta y_4) \tag{4}$$

where Δx_i and Δy_i are the relative displacements of the *i*-th node of the element, respectively.

The relative displacement vector $\boldsymbol{d}$ can be decomposed by using the base matrix $\mathbf{B}$, as follows,

$$\mathbf{B}\boldsymbol{d} = \begin{bmatrix} \mathbf{B}_r \\ \mathbf{B}_d \end{bmatrix} \boldsymbol{d} = \begin{bmatrix} \boldsymbol{p}_r \\ \boldsymbol{p}_d \end{bmatrix} \tag{5}$$

$$\boldsymbol{p}_r = \begin{bmatrix} p_1 \\ p_2 \\ p_3 \end{bmatrix} \tag{6}$$

where p_1, p_2 and p_3 are the projection coefficients of the rigid body linear displacement in X and Y directions, and relative rigid rotational displacement in XOY plane.

Comparing the absolute values of p_1, p_2 and p_3, the rigid body displacement corresponding to the projection coefficient with the largest absolute value was defined as the main rigid body displacement of the element. Yellow and green were assigned to represent the rigid body linear displacements in the X and Y directions, respectively, while blue was assigned to represent the rigid body rotational displacement in the XOY plane. By assigning the corresponding colors to each element, the relative rigid body displacement decomposition diagram was obtained, thereby enabling the visual analysis of the mode shapes of the timber pieces.

The X direction rigid body linear displacement coefficient of the timber pieces was obtained as follows,

$$D_x = \frac{n_x}{n_t} \quad (7)$$

where n_x is the number of elements dominated by the rigid body linear displacement in X direction, and n_t is the total number of elements. Similarly, the Y direction rigid body linear displacement coefficient D_y and the XOY plane rigid body rotational displacement coefficient R_{xoy} of the timber structure were obtained, thereby enabling the quantitative analysis of the mode shapes of the timber pieces.

EXPERIMENTAL SETUP

Material Parameters and Source

In this paper, the elastic modulus of the timber was 9 GPa along the grain, 0.5 GPa perpendicular to the grain, and the Poisson's ratio is 0.3. The parameters are taken from the conventional material properties of timber specified in Standard for Design of Timber Structures, GB/T 50005 (2017).

Finite Element Modeling Assumptions

The orthotropic mechanical behavior of timber was numerically simulated by defining distinct elastic modulus values for the finite element in the X and Y directions, respectively. In this numerical model, timber was assumed to be a purely elastic material, where plastic deformation and material damage were not taken into account. Additionally, the impacts of ambient environmental factors including temperature and relative humidity were excluded from the analysis.

Mesh and Calculation Settings

Timber pieces were modeled with 2D-4 node quadrilateral elements (ANSYS PLANE182). After conducting mesh convergence verification, an element size of 40 mm was determined for the numerical model. The Block Lanczos method was adopted to extract the mode shapes of the timber pieces.

EXAMPLE VERIFICATION

Planar Timber Column

A planar solid timber column with a fixed base and a free top was selected as the research example, which had a vertical height of 2000 mm and a square cross-section of 400×400 mm. The vertical axis of the column was aligned with the grain direction of the timber. A finite element model of the timber column was constructed in ANSYS, upon which modal analysis was subsequently conducted. The first eight mode shapes of the column are presented in Fig. 3. The mode shapes were decomposed using the method proposed in this paper, and the corresponding relative rigid body displacement decomposition diagrams were plotted, as shown in Fig. 4. The first three orders of mode shapes were used as examples to illustrate the recognition results of the two methods.

Figure 3a shows a timber column that exhibits an overall lateral bending deformation under the 1st mode shape. Combined with the mode shape mass participation ratio presented in Table 1, the 1st mode shape is identified as the first-order lateral bending

mode shape. It can be concluded from Fig. 4a and Table 1 that, except for the fixed end, the elements dominated by the X direction rigid body linear displacement (yellow area) almost cover the entire timber column, with the X direction rigid body linear displacement coefficient reaching 0.865. Therefore, the 1st mode shape can be identified as the first-order lateral bending mode shape.

Figure 3b shows a timber column that exhibits an overall lateral bending deformation under the 2nd mode shape, with an inflection point appearing in the mode shape. Combined with the mode shape mass participation ratio presented in Table 1, the 2nd mode shape is identified as the second-order lateral bending mode shape. It can be concluded from Fig. 4b and Table 1 that, except for the fixed end, the elements dominated by the X direction rigid body linear displacement (yellow area) almost cover the entire timber column, while elements dominated by the rigid body rotational displacement (blue area) emerge at the bending center. With the X direction rigid body linear displacement coefficient reaching 0.768, the 2nd mode shape can thus be identified as the second-order lateral bending mode shape.

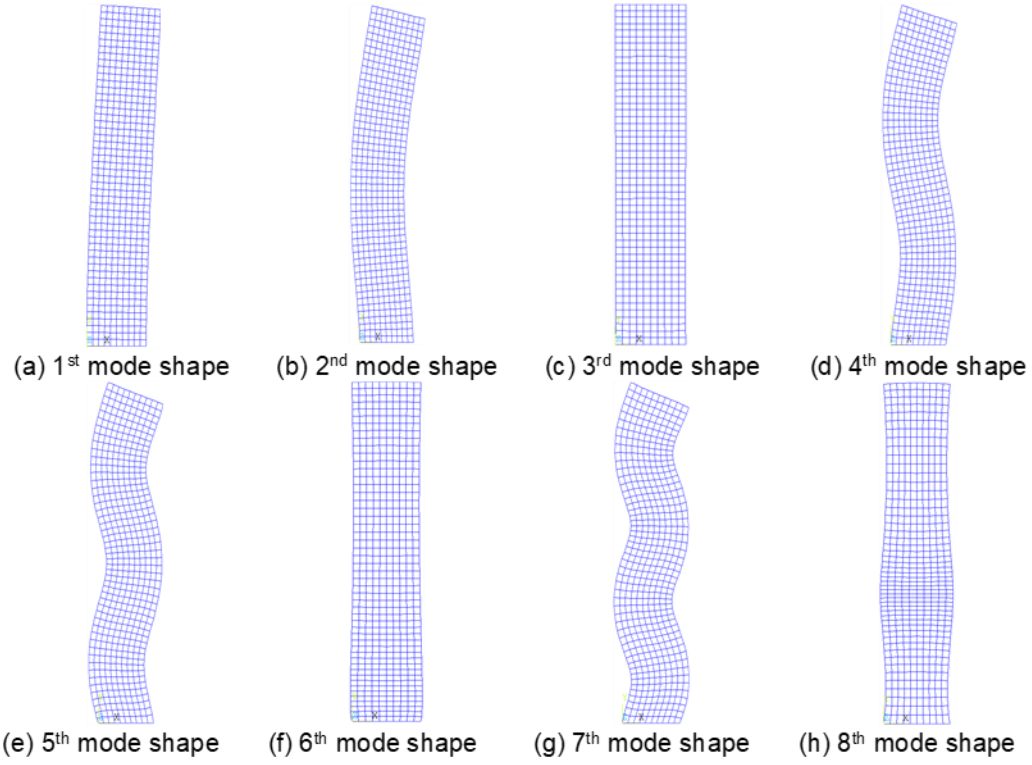

Fig. 3. Finite element mode shape diagrams of the timber column

Figure 3c shows a timber column that exhibits an overall vertical tension-compression deformation under the 3rd mode shape. Combined with the mode shape mass participation ratio presented in Table 1, the 3rd mode shape is identified as the first-order vertical tension-compression mode shape. It can be concluded from Fig. 4c and Table 1 that the elements dominated by the Y direction rigid body linear displacement (green area) almost cover the entire timber column, with the Y direction rigid body linear displacement coefficient reaching 0.985. Therefore, the 3rd mode shape can be identified as the first-order vertical tension-compression mode shape.

This case study demonstrates that the results of mode shape identification obtained by the method proposed in this paper are consistent with those derived from the traditional animation observation method and the modal mass participation ratio method (Wilson 2008).

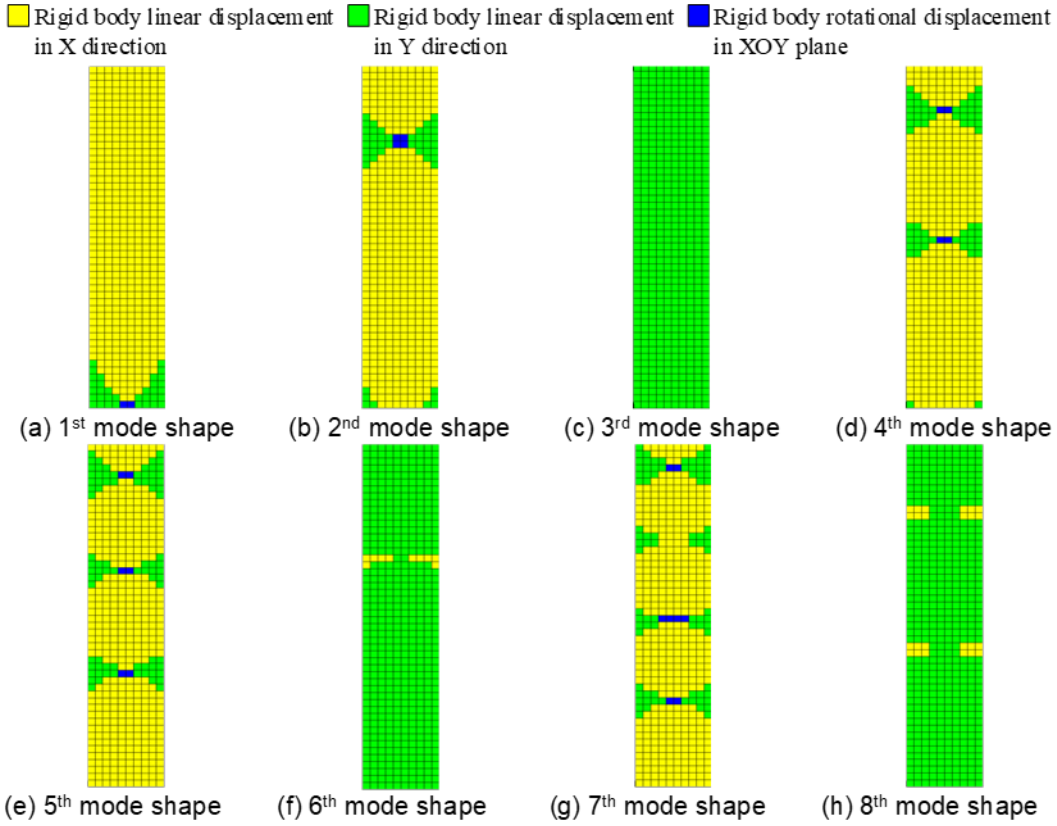

Fig. 4. Relative rigid body displacement decomposition diagrams of the timber column

A comparison of the mode shape identification results based on the modal mass participation ratio method and the relative rigid body displacement decomposition method is presented in Table 1. The variation trends of each rigid body displacement coefficient are consistent with those of the modal mass participation ratios in the X, Y, and Rot directions, and the mode shape descriptions are also identical, which verifies the validity of the mode shape identification results based on the rigid body displacement decomposition method. The relative rigid body displacement decomposition diagrams show that for the first-order lateral bending mode shape (Fig. 4a), the timber column has no inflection points except at the fixed end, and its elements are mainly dominated by the X direction rigid body linear displacement (yellow area). The second-order lateral bending mode shape (Fig. 4b) has one inflection point (green and blue areas); the third-order lateral bending mode shape (Fig. 4d) has two inflection points (green and blue areas), and so forth. The first-order vertical tension-compression mode shape (Fig. 4c) has no inflection points, with its elements mainly dominated by the Y direction rigid body linear displacement (green area). The second-order vertical tension-compression mode shape (Fig. 4f) has one inflection point (yellow area); the third-order vertical tension-compression mode shape (Fig. 4h) has two inflection points (yellow area). The relative rigid body displacement decomposition diagrams fully reflect the intuitiveness of mode shape identification. In

addition, the method proposed in this paper can also determine the dominant rigid body displacement type of each element in all mode shapes, which highlights its superiority.

Table 1. Comparison of Mode Shape Identification Results for the Timber Column between FEM and the Relative Rigid Body Displacement Decomposition Method

Mode shape	FEM				Relative Rigid Displacement Decomposition Method			
	Mass participation ratio in different directions			Mode shape description	Relative rigid displacement decomposition in different directions			Mode shape description
	X	Y	Rot		D_x	D_y	R_{xoy}	
1st	0.616	0.000	0.944	1st lateral bending	0.865	0.105	0.030	1st lateral bending
2nd	0.203	0.000	0.023	2nd lateral bending	0.768	0.177	0.055	2nd lateral bending
3rd	0.000	0.814	0.023	1st vertical tension-compression	0.015	0.985	0.001	1st vertical tension-compression
4th	0.071	0.000	0.003	3rd lateral bending	0.722	0.205	0.074	3rd lateral bending
5th	0.036	0.000	0.000	4th lateral bending	0.693	0.217	0.090	4th lateral bending
6th	0.000	0.090	0.003	2nd vertical tension-compression	0.047	0.950	0.004	2nd vertical tension-compression
7th	0.021	0.000	0.000	5th lateral bending	0.674	0.221	0.105	5th lateral bending
8th	0.000	0.032	0.001	3rd vertical tension-compression	0.089	0.900	0.011	3rd vertical tension-compression

Planar Timber Beam

To further validate the method's universality, a planar simply supported timber beam (1920 mm in length, 480 mm in height, 300 mm in thickness) was analyzed, with the length direction as the timber grain direction.

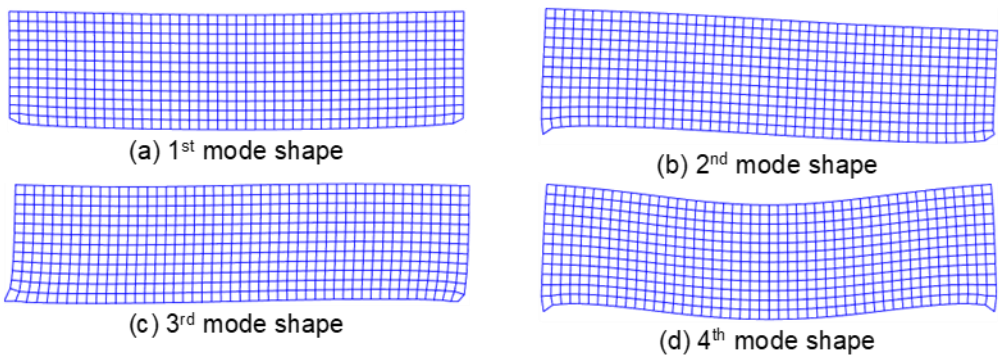

Fig. 5. Finite element mode shape diagrams of the timber beam

Its first four mode shapes are given in Fig. 5, and the corresponding relative rigid body displacement decomposition diagrams in Fig. 6. Table 2 presents the identification results obtained by the modal mass participation ratio method and the relative rigid body displacement decomposition method.

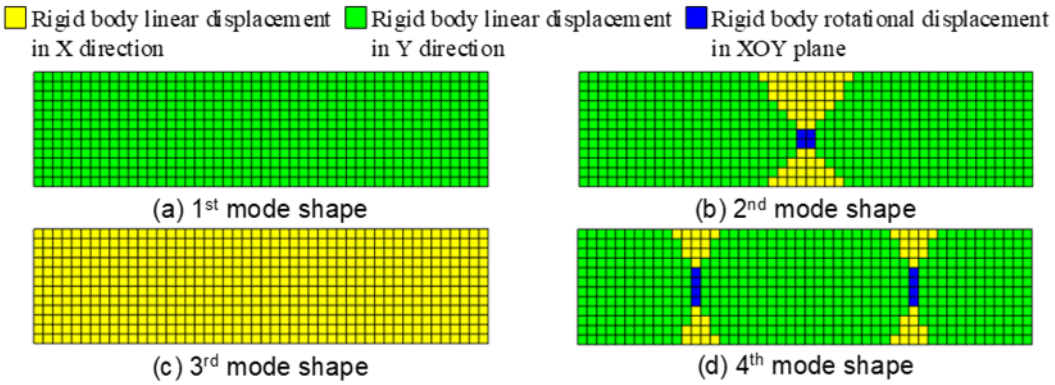

Fig. 6. Relative rigid body displacement decomposition diagrams of the timber beam

Table 2. Comparison of Mode Shape Identification Results for the Timber Beam between FEM and the Relative Rigid Body Displacement Decomposition Method

Mode shape	FEM				Relative Rigid Displacement Decomposition Method			
	Mass participation ratio in different directions			Mode shape description	Relative rigid displacement decomposition in different directions			Mode shape description
	X	Y	Rot		D_x	D_y	R_{xoy}	
1st	0.000	0.913	0.690	1st vertical bending	0.000	1.000	0.000	1st vertical bending
2nd	0.004	0.050	0.258	2nd vertical bending	0.101	0.892	0.007	2nd vertical bending
3rd	0.965	0.000	0.032	1st lateral shear	1.000	0.000	0.000	1st lateral shear
4th	0.000	0.026	0.013	3rd vertical bending	0.076	0.910	0.014	3rd vertical bending

Under the 1st mode shape, the timber beam exhibited an overall vertical bending deformation (Fig. 5a). Combined with the modal mass participation ratios in Table 2, the 1st mode shape was identified as the 1st vertical bending mode shape. As can be seen from Fig. 6a, all elements of the timber beam were dominated by Y direction rigid body linear displacement (green elements), with the Y direction rigid body linear displacement coefficient being 1. Therefore, the mode shape identification results based on the relative rigid body displacement decomposition method were consistent with those of the modal mass participation ratio method. By the same token, the 2nd to 4th mode shapes were identified as the 2nd vertical bending mode shape, the 1st lateral shear mode shape, and the 3rd vertical bending mode shape, respectively.

The above results indicate that the mode shape identification method based on relative rigid body displacement decomposition exhibits good applicability to different types of timber pieces.

CONCLUSIONS

1. Based on the deformation decomposition theory of 2D-4 node quadrilateral elements, a relative rigid body displacement decomposition method for mode shapes of timber pieces was established to realize quantitative mode shape identification.
2. Verified through comparison with the traditional finite element animation method and the modal mass participation ratio method, the proposed method yielded consistent results while possessing the advantages of both quantitative accuracy and visualization. It can determine the dominant rigid body displacement type of each element.
3. The proposed method can rapidly identify the mode shapes of timber pieces, providing a reliable basis for seismic design, health monitoring, and damage identification. The visualized decomposition diagrams enable engineers to intuitively judge the weak regions of pieces, reduce subjective identification errors, and are applicable to dynamic characteristic analysis of various timber pieces.

ACKNOWLEDGMENTS

This work was supported by the China Postdoctoral Science Foundation (Grant No. 2025T180893), Science and Technology Research Project of Henan Province (Grant No. 252102321013), Young Elite Scientists Sponsorship Program by Henan Association for Science and Technology (Grant No. 2025HYTP009) and Postdoctoral Research Foundation of Henan Province (Grant No. HN2025034).

REFERENCES CITED

Amaddeo, C., and Martinelli, M. D. L. (2025), "Initial monitoring of a six-story lightweight timber frame building under different environmental conditions," *Journal of Civil Structural Health Monitoring* 15(2), 371-393. https://doi.org/10.1007/s13349-024-00867-w

Augustino, D. S. (2025). "Potential of sustainable timber modular houses in southern highland, Tanzania: The structural response of timber modules under wind load," *Buildings* 15, article 1459. https://doi.org/10.3390/buildings15091459

Bracci, J. M., and Kunnath, S. K. (1997). "Seismic performance and retrofit evaluation of reinforced concrete structures," *Journal of Structural Engineering* 123(1), 3-10. https://doi.org/10.1061/(ASCE)0733-9445(1997)123:1(3)

Caprio, D., and Jockwer, R. (2026). "Impact of steel-to-timber joints with screws on the failure modes and reliability of a structurally indeterminate timber beam," *Engineering Structures* 349, article e121883. https://doi.org/10.1016/j.engstruct.2025.121883

Casalegno, C., and Russo, S. (2017). "Dynamic characterization of an All-FRP bridge," *Mechanics of Composite Materials* 53, 17-30. https://doi.org/10.1007/s11029-017-9637-0

Cheraghi-Shirazi, N., Creagh, A., Setiawan, F., Parra, R., Khoshkbari, P. and Malek, S. (2025). "A numerical modelling framework for vibration assessment of timber

composite floors in mass timber buildings," *Journal of Building Engineering* 106, article 112605. https://doi.org/10.1016/j.jobe.2025.112605

Gao, L. L., Yu, H. F., Huang, H., Duan, P. B., and Ma, K. (2025). "Study on seismic performance of post-and-lintel timber structure," *Structures* 82, article 110628. https://doi.org/10.1016/j.istruc.2025.110628

GB/T 50005 (2017). "Standard for design of timber structures," Standardization Administration of China, Beijing, China.

Ghiyasinasab, M., Lehoux, N., and Menard, S. (2017). "Production phases and market for timber gridshell structures: A state-of-the-art review," *BioResources* 12(4), 9538-9555. https://doi.org/10.15376/biores.12.4.Ghiyasinasab

Hamdi, S. E., Sbartaï, Z. M., and Elachachi, S. M. (2021). "Performance assessment of modal parameters identification methods for timber structures evaluation: Numerical modeling and case study," *Wood Science and Technology* 55, 1593-618. https://doi.org/10.1007/s00226-021-01335-0

Jara-Cisterna, A., Benedetti, F., Rosales, V., Almazán, J. L. and Opazo-Vega, A. (2025), "Vibration-based monitoring of a cross-laminated timber building in a high seismicity zone," *Journal of Civil Structural Health Monitoring* 15(2), 333-353. https://doi.org/10.1007/s13349-024-00862-1

Pan, Y., Yi, D. H., Khennane, A., and Chen, J. (2023). "Seismic performance of a historic timber structure on a slope," *Journal of Building Engineering* 71, article 106434. https://doi.org/10.1016/j.jobe.2023.106434

Patil, K., Srivastava, V., and Baqersad, J. (2018). "A multi-view optical technique to obtain mode shapes of structures," *Measurement* 122, 358-367. https://doi.org/10.1016/j.measurement.2018.02.059

Perlin, L. P., Pinto, R. C. D. A., and Valle, Â. D. (2019). "Ultrasonic tomography in wood with anisotropy consideration," *Construction and Building Materials* 229, article 116958. https://doi.org/10.1016/j.conbuildmat.2019.116958

Ren, X. C., Meng, Z. B., Wu, Y. J., Xie, Q. F., Liu, Y. J., and Wang, X. (2025). "Seismic performance of traditional Chinese timber structure: A case of guangyue tower," *Journal of Building Engineering* 100, article 111690. https://doi.org/doi.org/10.1016/j.jobe.2024.111690

Renard, S., Robert, F., Franssen, J., Zehfuss, J., McNamee, R., Bamonte, P., and Gernay, T. (2025). "Structural behavior of timber columns in wood crib compartment fire tests," *Fire Safety Journal* 155, article 104413. https://doi.org/10.1016/j.firesaf.2025.104413

Sejkot, P., Aloisio, A., De Santis, Y., Fragiacomo, M., and Iqbal, A. (2025). "Overstrength and variance analysis of angle brackets for timber structures considering the uncertainty in the nail-timber interaction," *Journal of Building Engineering* 113, article 113991. https://doi.org/10.1016/j.jobe.2025.113991

Sun, P. X., Li, K. G., and Sun, G. Z. (2023). "Comparative analysis of mechanical properties for wood frame and reinforced concrete frame based on deformation energy decomposition method," *BioResources* 18(4), 7124-7142. https://doi.org/10.15376/biores.18.4.7124-7142

Sun, P. X., Nie, P. J., Liang, K. X. and Wang, D. W. (2025), "The performance analysis of shear walls with opening based on quantitative identification method of vibration modes," *Alexandria Engineering Journal* 120, 637-647. https://doi.org/10.1016/j.aej.2025.02.074

Véliz, F., Chacón, M. F., Lagos, J., Berwart, S., López, N., and Guindos, P. (2024). "Structural performance of strong timber diaphragms: High-capacity light-timber frames and cross-laminated timber," *Structures* 63, article 106335. https://doi.org/10.1016/j.istruc.2024.106335

Wilson, E. L. (2008). *Three Dimensional Static and Dynamic Analysis of Structures: A Physical Approach with Emphasis on Earthquake Engineering*, Computers and Structures, Inc., Berkeley, CA, USA.

Xu, Q. Y., Zou, H. Y., Wang, Z., He, Y. H., Qi, L., and Wang, J. (2024). "Modal testing and analysis of high-rise laminated timber building," *BioResources* 19(4), 9616-9630. https://doi.org/10.15376/biores.19.4.9616-9630

Yassine, R., and Mustapha, S. (2024). "The effect of moisture content and temperature on the propagation characteristics of guided waves in timber utility poles-numerical and experimental validation," *Wood Science and Technology* 58(2), 533-573. https://doi.org/10.1007/s00226-023-01528-9

Zhao, K., Ge, Z. D., Huo, L. L., Gao, Y. S., and Yao, Y. C. (2024). "Application progress and prospect of defect detection technology for timber structure members," *Russian Journal of Nondestructive Testing* 60, 455-69. https://doi.org/10.1134/S1061830924600217

Article submitted: January 19, 2026; Peer review completed: March 15, 2026; Revised version received and accepted: March 29, 2026; Published: April 9, 2026.
DOI: 10.15376/biores.21.2.4666-4677